Improving Depiction of Temporal Bone Anatomy With Low-Radiation Dose CT by an Integrated Circuit Detector in Pediatric Patients

A Preliminary Study

Jingzhen He, MD, PhD, Yuliang Zu, MD, Qing Wang, MD PhD, and Xiangxing Ma, MD

Abstract: The purpose of this study was to determine the performance of low-dose computed tomography (CT) scanning with integrated circuit (IC) detector in defining fine structures of temporal bone in children by comparing with the conventional detector.

The study was performed with the approval of our institutional review board and the patients' anonymity was maintained. A total of 86 children <3 years of age underwent imaging of temporal bone with low-dose CT (80 kV/150 mAs) equipped with either IC detector or conventional discrete circuit (DC) detector. The image noise was measured for quantitative analysis. Thirty-five structures of temporal bone were further assessed and rated by 2 radiologists for qualitative analysis. κ Statistics were performed to determine the agreement reached between the 2 radiologists on each image. Mann–Whitney U test was used to determine the difference in image quality between the 2 detector systems.

Objective analysis showed that the image noise was significantly lower ($P < 0.001$) with the IC detector than with the DC detector. The κ values for qualitative assessment of the 35 fine anatomical structures revealed high interobserver agreement. The delineation for 30 of the 35 landmarks (86%) with the IC detector was superior to that with the conventional DC detector ($P < 0.05$) although there were no differences in the delineation of the remaining 5 structures ($P > 0.05$).

The low-dose CT images acquired with the IC detector provide better depiction of fine osseous structures of temporal bone than that with the conventional DC detector.

Abbreviations: ADCs = analog-to-digital converters, CTDIvol = volume CT dose index, DC = discrete circuit, DLP = dose length product, IC = integrated circuit, MSCT = multislice computed tomography, SD = standard deviation.

INTRODUCTION

Multislice computed tomography with high spatial resolution plays an important role in the imaging delineation of temporal bone.[1–3] With the advance of computed tomography (CT) technology, a sharp increase in CT scan use has been observed in recent years.[4] Consequently, there is a growing concern regarding the potential risks of radiation exposure, particularly for children, and various methods and strategies based on individual patient attributes and CT technology have been explored to decrease the radiation dose level during the imaging of temporal bone.[5–10]

Recently, a CT scanner employing an integrated circuit (IC) detector potentially reducing image noise and improving spatial resolution by means of reduced crosstalk between detector channels was introduced into clinical practice. Unlike the discrete circuit (DC) system of conventional CT detector technology, this new type of detector combines the photodiodes and the analog-to-digital converters (ADCs) on a single board into an IC detector. This reduces the transmission time of analog signal, thus reducing the power consumption, heat dissipation, and electronic noise. As a result, the IC detector technology lowers the image noise by means of reduced loss of information during the transfer of analog-to-digital signals compared with DC detector technology.[11,12] The IC detector technology is considered to be particularly useful for low-dose CT scans because electronic noise becomes more and more dominant with decrease in the amount of detected photons.[13]

The present study was designed to evaluate the quality of images acquired with low-dose CT equipped with the IC detector through comparative analysis between the IC and conventional DC detectors in respect of the depiction of anatomic landmarks of the temporal bone in pediatric patients.

MATERIALS AND METHODS

Patients and CT Scanning Protocol

This retrospective study was approved by our institutional review board with written informed consent waived. From October 2013 to May 2014, 86 consecutive low-dose CT examinations were performed in patients <3 years of age with clinical signs suspicious for various inner and middle ear abnormalities were selected upon reviewing electronic medical records of our hospital. Of them, 48 patients were scanned on a 128-slice CT scanner equipped with a conventional DC detector (Somatom Definition Flash; Siemens Healthcare, Forchheim, Germany) and the other 38 patients were imaged on a similar CT scanner equipped with an IC detector (Stellar; Siemens Healthcare, Erlangen, Germany). Exclusion criteria consisted of

any evidence of severe abnormalities of temporal bone (such as middle/inner ear dysplasia or trauma, or infectious conditions leading to destruction of the skull base, or patients with electric devices at the skull base) affecting anatomic evaluation established by 2 radiologists who did not involve in the further studies. With the criteria, 16 (6 with IC and 10 with conventional DC detector) patients were excluded because of tympanitis with erosion of auditory ossicles ($n = 10$), middle ear dysplasia ($n = 2$), and cochlea implants ($n = 4$). Finally, a total of 140 temporal bone studies of 70 patients were included in the study; 38 patients including 20 males and 18 females (mean age, 9 months; range, 3 months to 3 years) were scanned on the CT scanner equipped with a conventional DC detector and the other 32 patients including 18 males and 14 females (mean age, 10 months; range, 2 months to 3 years) were imaged on a similar CT scanner equipped with an IC detector.

The scanning parameters were the same for both detectors: slice acquisition was $2 \times 0.6 \times 64$, by means of a z-flying focal spot; gantry rotation, 0.5 seconds; tube voltage, 80 kV; and tube current–time product, 150 effective mAs. All images were reconstructed using a sharp kernel (B60) with a field of view of 100 mm and with a slice thickness of 0.6 mm and an increment of 0.4 mm.

Image Evaluation

The reading sessions were done on a picture archiving and communication system workstation using axial sections and multiplanar reformations generated with the integrated software tools. Two radiologists (12 and 10 years of experience in interpreting head and neck imaging, respectively) who were unaware of the CT scanning parameters reviewed the images independently. In accordance with our clinical routine, reviewers were free to choose the appropriate planes and all images were displayed at a window level of 800 Hounsfield units (HU) and a window width of 4000 HU.

To quantitatively evaluate the image quality, we measured the image noise (standard deviation [SD] of the CT number in HU) of the brain stem region by placing circular regions of interest of 50 mm^2. For subjective analysis, 2 reviewers evaluated the image quality with respect to the visibility of 35 anatomic landmarks (Table 1) by using 5-point quality rating: 1, anatomic structures not identifiable because of poor image quality; 2, structures identifiable, but no details assessable, resulting in insufficient image quality; 3, anatomic structures still fully assessable in all parts and acceptable image quality; 4, clear delineation of structure and good image quality; and 5, very good delineation of structure and excellent image quality.[10] The summed score for the 35 structures in each ear was correspondingly calculated.

Statistical Analysis

The statistical analyses were performed with the statistical software of SPSS (version 19.0, SPSS Inc, Chicago, IL) for Microsoft Windows. For the continuous variables, Kolmogorov–Smirnov test was applied to assess the normality of data distribution, and Levene test was used to evaluate the equality of variance. Patients' ages of the IC and the DC detector groups were compared using independent t test, and the sex composition using Fisher exact test. For the quantitative analysis, the image noise was expressed as mean $\pm$ SD and the intergroup difference for each category was tested with the unpaired t test. For the qualitative analysis, the differences for the subjective scores of the images acquired by 2 detector

TABLE 1. κ Values for the 2 Observers Who Evaluated the Image Quality

Anatomical Structures	DC Detector	IC Detector
Tympanic membrane	0.88	0.91
Facial nerve canal: labyrinthine segment S1	0.99	0.94
Facial nerve canal: tympanic segment S2	0.87	1.00
Facial nerve canal: mastoid segment S3	0.85	0.87
Canal of the cochlear nerve	0.91	0.88
Canal of the superior division of the vestibular nerve	1.0	0.82
Canal of the inferior division of the vestibular nerve	0.93	0.98
Malleus head	0.84	0.99
Malleus neck	0.88	0.86
Manubrium of malleus	0.85	0.92
Lateral process of malleus	0.94	0.93
Anterior process of malleus	0.90	0.91
Incus body	1.00	0.89
Short process of incus	0.99	1.00
Long process of incus	0.98	0.86
Lenticular process of incus	0.97	0.88
Incudomalleolar articulation	0.96	0.90
Stapes head	0.91	0.95
Anterior crus of stapes	0.87	0.86
Posterior crus of stapes	1.00	0.88
Stapes footplate	0.86	0.96
Incudostapedial articulation	0.99	0.97
Oval window	0.90	0.97
Round window	0.84	0.93
Pyramidal eminence	0.91	1.00
Osseous spiral lamina of cochlea	0.84	0.90
Modiolus of cochlea	0.92	0.94
Cochlear aqueduct	0.96	0.85
Vestibular aqueduct	0.89	1.00
Stapedius muscle	0.88	0.90
Tegmen tympani	0.90	1.00
Vestibule	0.91	0.94
Horizontal semicircular canal	0.93	0.97
Superior semicircular canal	1.00	0.89
Posterior semicircular canal	0.98	0.87

DC = discrete circuit, IC = integrated circuit.

systems were tested with the Mann–Whitney U test. Inter-reader variability for the subjective evaluation of image quality was assessed with the κ statistics. The κ values of ≤ 0.4 were considered to indicate positive but poor agreement, while the values of 0.41–0.75 and >0.75 indicated good and excellent agreement.

RESULTS

No statistical differences in age and sex composition were found between IC and DC detectors ($P > 0.05$). There was a significantly lower image noise in datasets acquired with the IC compared with the DC detector ($P < 0.001$). The mean (SD)

image noise was 56.6 versus 46.0 HU for the DC versus IC detector. The overall noise reduction was up to 19% for the images acquired with the IC detector compared with the DC detector.

The κ values for qualitative assessment revealed a high interobserver agreement for all 35 fine anatomical structures, showing a mean of 0.94 (range, 0.82–1.0) for images acquired with IC detector and 0.96 (range, 0.85–1.0) for images acquired with DC detector. Table 1 shows the κ values for the 2 observers who evaluated the CT images, and Table 2 summarizes the mean ± SD scores of image quality and the *P* values.

With respect to the visibility of temporal bone, the mean subjective scores of images acquired with IC detector were superior to the scores with conventional DC detector for all of the 35 structures. Significant differences were obtained for 30 of the 35 structures in the anatomy depiction between IC and DC detectors ($P < 0.05$). No difference was observed between the IC and conventional DC detectors ($P > 0.05$) for delineation of the remaining 5 structures including the horizontal semicircular canal, superior semicircular canal, posterior semicircular canal, vestibule, and incus body.

DISCUSSION

Our study demonstrated that use of the IC detector improved the image quality with respect to the depiction of anatomic landmarks of pediatric temporal bone as compared with the use of the conventional DC detector in low-dose CT. In our low-dose CT protocol, 80 kV and 150 mAs were used. The mean values of volume CT dose index (CTDIvol, mGy) and dose length product (DLP, mGy●cm) provided by the CT scanner were 9.8 and 42, respectively. The CTDIvol and DLP of this low-dose protocol were approximately 5 and 4 times lower, respectively, than that of standard-dose protocol (120 kV, 200 mAs).[9,10]

In the acquisition of CT data, the image noise mainly comes from quantum noise from photon statistics and electronic noise associated with the photon detection system, or CT detectors. Electronic noise usually has a minor effect on the image quality in the case of routine dose CT scanning. However, the amount of detected photons can decrease to a level at which the signal from the photons is comparable to the electronic noise for low-dose CT scanning.[13] Compared with

TABLE 2. Mean Scores and *P* Values for Qualitative Analysis of the Image Quality Between the 2 Detector Systems

Anatomical Structures	DC Detector	IC Detector	*P*
Tympanic membrane	4.25 ± 0.85	4.43 ± 0.62	0.004
Facial nerve canal: labyrinthine segment S1	4.06 ± 0.83	4.35 ± 0.65	0.023
Facial nerve canal: tympanic segment S2	4.10 ± 0.65	4.45 ± 0.71	0.036
Facial nerve canal: mastoid segment S3	4.05 ± 0.79	4.36 ± 0.82	0.001
Canal of the cochlear nerve	4.35 ± 0.64	4.45 ± 0.75	0.026
Canal of the superior division of the vestibular nerve	4.25 ± 0.65	4.36 ± 0.65	0.002
Canal of the inferior division of the vestibular nerve	4.16 ± 0.65	4.27 ± 0.65	0.032
Malleus head	4.45 ± 0.98	4.68 ± 0.25	0.034
Malleus neck	4.63 ± 0.43	4.65 ± 0.90	0.030
Manubrium of malleus	4.39 ± 0.68	4.43 ± 0.76	0.024
Lateral process of malleus	4.31 ± 1.05	4.49 ± 0.65	0.013
Anterior process of malleus	3.25 ± 0.42	3.65 ± 0.87	0.034
Incus body	4.68 ± 0.73	4.79 ± 0.86	0.99
Short process of incus	4.25 ± 0.65	4.51 ± 0.45	0.047
Long process of incus	4.35 ± 0.65	4.39 ± 0.65	0.033
Lenticular process of incus	3.25 ± 0.95	3.66 ± 0.76	0.003
Incudomalleolar articulation	3.72 ± 0.85	3.84 ± 0.95	0.012
Stapes head	3.44 ± 0.65	3.62 ± 0.74	0.034
Anterior crus of stapes	4.05 ± 0.59	4.32 ± 0.48	0.026
Posterior crus of stapes	4.08 ± 0.71	4.21 ± 0.83	0.007
Stapes footplate	3.27 ± 0.91	3.65 ± 0.65	0.004
Incudostapedial articulation	3.61 ± 0.74	3.72 ± 0.83	0.035
Oval window	4.05 ± 0.65	4.37 ± 0.76	0.024
Round window	3.25 ± 0.83	3.56 ± 0.92	0.014
Pyramidal eminence	4.05 ± 0.72	4.46 ± 0.83	0.010
Osseous spiral lamina of cochlea	4.11 ± 0.71	4.37 ± 0.85	0.027
Modiolus of cochlea	4.12 ± 0.65	4.36 ± 0.91	0.036
Cochlear aqueduct	4.75 ± 0.46	4.86 ± 0.57	0.028
Vestibular aqueduct	4.05 ± 0.98	4.23 ± 0.85	0.044
Stapedius muscle	4.63 ± 0.79	4.72 ± 0.64	0.039
Tegmen tympani	4.59 ± 0.72	4.61 ± 0.68	0.021
Vestibule	4.67 ± 0.64	4.68 ± 0.59	0.38
Horizontal semicircular canal	4.82 ± 0.55	4.85 ± 0.65	0.66
Superior semicircular canal	4.73 ± 0.65	4.81 ± 0.65	0.82
Posterior semicircular canal	4.70 ± 0.72	4.86 ± 0.61	0.94

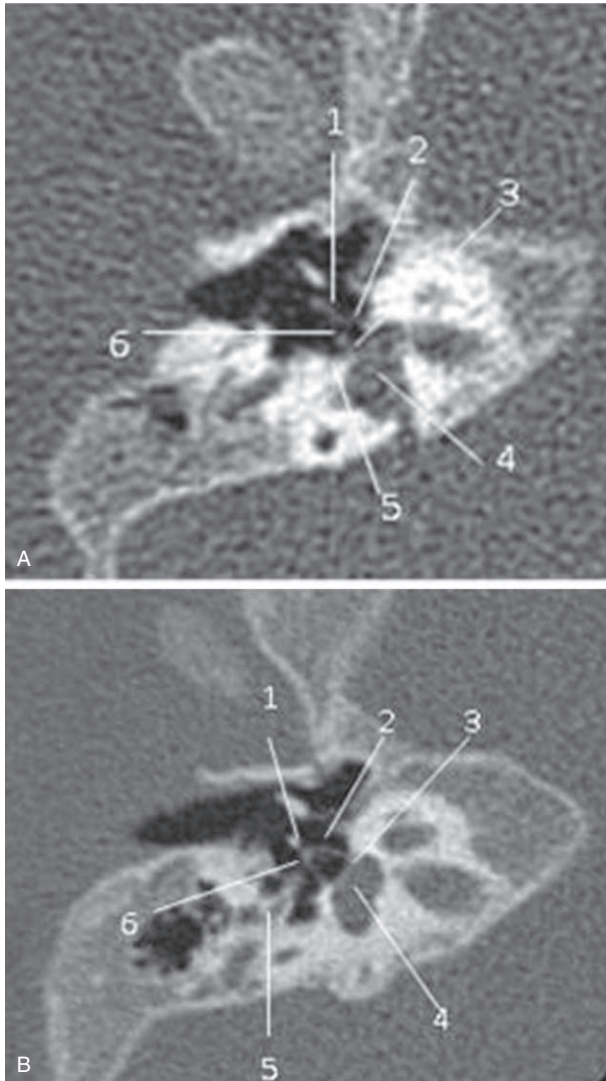DC = discrete circuit, IC = integrated circuit.

FIGURE 1. Oblique axial images reformatted in the stapes main plane obtained with (A) conventional (16-month-old child) and (B) integrated circuit (IC) detectors (16-month-old child). Critical structures such as the stapes head (1), anterior crus of stapes (2), oval window (3), vestibule (4), stapedius muscle (5), and posterior crus of stapes (6) are better delineated with IC detector.

FIGURE 2. Oblique coronal reformatted images in cochlea plane with (A) conventional (16-month-old child) and (B) integrated circuit (IC) detectors (16-month-old child). Critical structures such as the vestibule (1), osseous spiral lamina of cochlea, and cochlear window (3) are better delineated with IC detector.

standard detector with ADC installed on a separate board, the photodiode and ADC in the IC detector are integrated into the same silicon chip that is attached to the backside of scintillating ceramic detector. The integration of the electronics with the detector element reduces the time during which the signal is in analog form, thereby reducing the amount of electronic noise that is added to the signal.[11–13]

The temporal bone is ideally suited for low-dose CT because of the high intrinsic contrast of the osseous structures surrounded by air component.[10,14,15] Low-dose CT of temporal bone is mainly used for preoperative assessment of the anatomy in the diagnosis of middle and inner ear dysplasia and the selection of cochlear implant candidates for children <3 years old in our hospital based our experience and manufacturer's recommendation. A prior study has reported that the normal temporal bone anatomy in young children using 80 kV could be
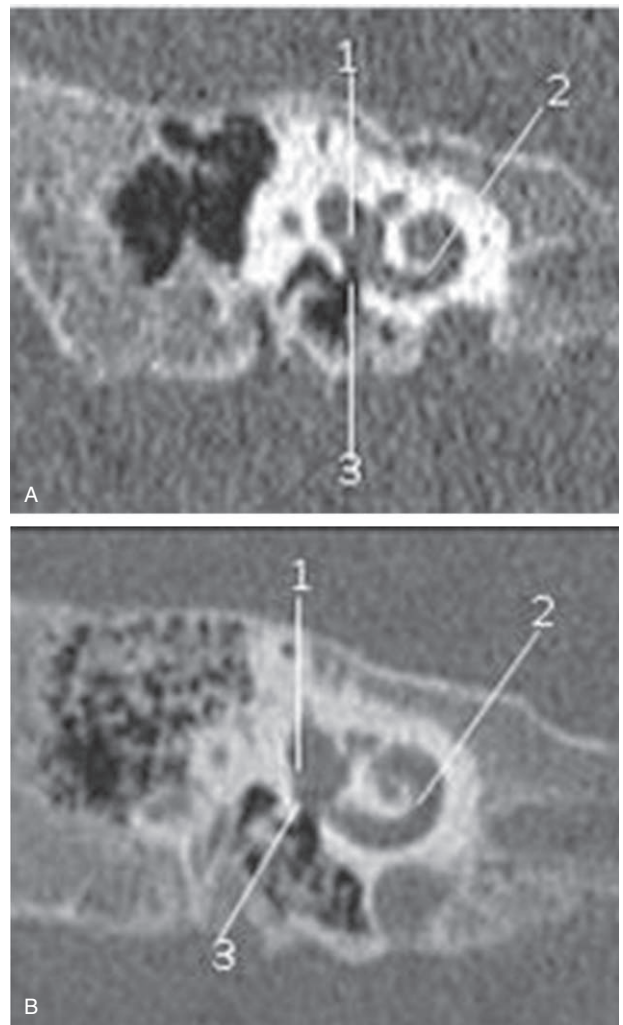
adequately assessed by radiologists but not by otologists with a significant reduction in radiation exposure compared with the previously used high-dose protocol.[10] In that study, the image quality was qualitatively assessed only by using a 5-point scale, no quantitative methods were applied.[10] In the present study, we applied both quantitative and qualitative methods to assess the quality of images obtained with the 2 detector systems. The image noise was reduced by 19% with the IC detector. Furthermore, 86% of the temporal bone landmarks were significantly delineated by the using of IC detector, superior to the conventional detector. In particular, the anatomical structures that are crucial for diagnosis of auditory ossicular dysplasia and inner ear surgery such as the ossicular chain and modulus were better delineated with the IC detector (Figures 1–3). In the remaining 14% landmarks, the mean score of image quality acquired by IC detector was also higher than that by conventional DC detector although there was no significant difference. Better objective and subjective image quality was achieved with the IC detector, suggesting that further dose-reduction methods
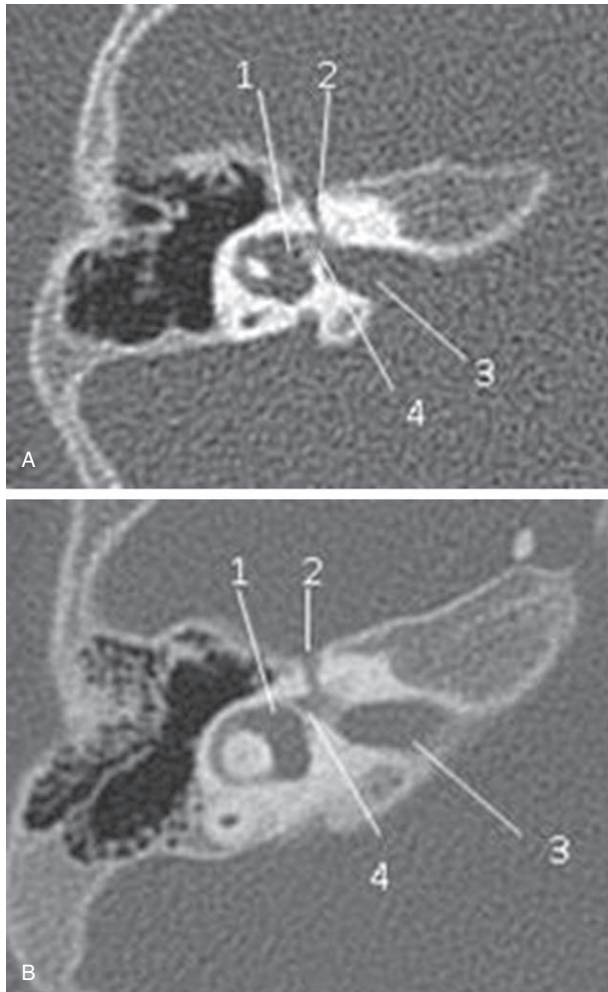
FIGURE 3. Axial reformatted images in internal auditory canal plane obtained with (A) conventional (12-month-old child) and (B) integrated circuit (IC) detectors (12-month-old child). Critical structures such as the vestibule (1), labyrinthine segment of facial nerve canal (2), internal auditory canal (3), and canal of the inferior division of the vestibular nerve (4) are better delineated with IC detector.

may be applied with comparable image quality by the use of IC detector.

The present study aimed to evaluate the image quality with respect to the delineation of temporal bone by 2 different detector technologies. We did not assess the relative values of the 2 detectors for specific diseases. The main purpose of this study was to gain insight into the potential for further dose

reduction in temporal CT. Focused studies with selected participant populations are ongoing in the pathologic conditions of temporal bone. Our preliminary data showed that the image quality acquired with IC detector was superior to that with conventional DC detector, suggesting that this technology is feasible for imaging of different disease categories and enables imaging with comparable quality at even lower radiation dose.

REFERENCES

1. Torizuka T, Hayakawa K, Satoh Y, et al. High-resolution CT of the temporal bone: a modified baseline. *Radiology.* 1992;184:109–111.

2. Caldemeyer KS, Sandrasegaran K, Shi-naver CN, et al. Temporal bone: comparison of isotropic helical CT and conventional direct transverse and coronal CT. *Am J Roentgenol.* 1999;172:1675–1682.

3. Jäger L, Bonell H, Liebl M, et al. CT of the normal temporal bone: comparison of multi- and single-detector row CT. *Radiology.* 2005;235:133–141.

4. Brenner DJ, Hall EJ. Computed tomography – an increasing source of radiation exposure. *N Engl J Med.* 2007;357:2277–2284.

5. Cohnen M, Fischer H, Hamacher J, et al. CT of the head by use of reduced current and kilovoltage: relation between image quality and dose reduction. *Am J Neuroradiol.* 2000;21:1654–1660.

6. Kalra MK, Maher MM, Toth TL, et al. Strategies for CT radiation dose optimization. *Radiology.* 2004;230:619–628.

7. McCollough CH, Primak AN, Braun N, et al. Strategies for reducing radiation dose in CT. *Radiol Clin North Am.* 2009;47:27–40.

8. Lutz J, Jäger V, Hempel MJ, et al. Delineation of temporal bone anatomy: feasibility of low-dose 64-row CT in regard to image quality. *Eur Radiol.* 2007;17:2638–2645.

9. Nauer CB, Zubler C, Weisstanner C, et al. Radiation dose optimization in pediatric temporal bone computed tomography: influence of tube tension on image contrast and image quality. *Neuroradiology.* 2012;54:247–254.

10. Nauer CB, Rieke A, Zubler C, et al. Low-dose temporal bone CT in infants and young children: effective dose and image quality. *Am J Neuroradiol.* 2011;32:1375–1380.

11. Morsbach F, Bickelhaupt S, Rätzer S, et al. Integrated circuit detector technology in abdominal CT: added value in obese patients. *Am J Roentgenol.* 2014;202:368–374.

12. Morsbach F, Desbiolles L, Plass A, et al. Stenosis quantification in coronary CT angiography: impact of an integrated circuit detector with iterative reconstruction. *Invest Radiol.* 2013;48:32–40.

13. Liu Y1, Leng S, Michalak GJ, et al. Reducing image noise in computed tomography (CT) colonography: effect of an integrated circuit CT detector. *J Comput Assist Tomogr.* 2014;38:398–403.

14. Singh S, Kalra MK, Moore MA, et al. Dose reduction and compliance with pediatric CT protocols adapted to patient size, clinical indication, and number of prior studies. *Radiology.* 2009;252:200–208.

15. Husstedt HW, Prokop M, Dietrich B, et al. Low-dose high-resolution CT of the petrous bone. *J Neuroradiol.* 2000;27:87–92.